

# 'Small Bodies: Near and Far' database of thermal infrared measurements of small Solar System bodies

Release Note: Public Release 1.2, 2019 March 29

Cs. Kiss<sup>1</sup>; R. Szakáts<sup>1</sup>, G. Marton<sup>1</sup>, A. Farkas-Takács<sup>1</sup>, T. Müller<sup>2</sup>, and V. Ali-Lagoa<sup>2</sup>

<sup>1</sup>Konkoly Observatory, Research Centre for Astronomy and Earth Sciences, Hungarian Academy of Sciences, Budapest, Hungary

<sup>2</sup>Max-Planck-Institut für extraterrestrische Physik, Garching, Germany

## 1 Introduction

A primary goal of the 'Small Bodies: Near and Far' infrared database is to help scientists working in the field of modeling the thermal emission of small bodies, providing them with an easy-to-use tool. Our database collects available thermal emission measurements for small Solar Systems targets that are otherwise available in scattered sources and gives a complete description of the data, with all information necessary to perform direct scientific calculations and without the need to access additional, external resources. The DB provides disk-integrated, calibrated flux densities based on careful considerations of instrument-/project-specific calibration and processing steps. These multi-epoch, multi-wavelength, multi-aspect data allow for a more complex thermophysical analysis for individual objects (e.g. using more sophisticated spin-shape solutions) or samples of objects. It will also allow to combine remote with close-proximity data for the same target. In addition to answering direct scientific questions related e.g. to thermal inertia and other surface properties of the targets it will also help in establishing celestial calibrators for instruments working in the thermal infrared regime, from mid-IR to submm wavelengths. At a later stage we aim to include thermal data for all Solar System small bodies which have been detected at thermal IR wavelengths.

The Infrared Database is part of the Horizon 2020 project 'Small Bodies: Near and Far' (COMPET-05-2015/687378).

---

### Version history:

Version	Date	Comment
V1.0	2019 February 12	original release (Thermops III version)
V1.1	2019 March 7	small text corrections
V1.2	2019 March 29	Herschel space observatory measurements added to the public database (this release, see the relevant items in the text)
V1.3	2021 February 2	More Herschel space observatory measurements added to the public database. Added description of alternative accessing methods.

## 2 Thermal infrared observations of asteroids and transneptunian objects

The main entries in our database are the (calibrated) infrared flux densities and the corresponding flux density error (denoted as  $f \pm df$  in the outline figure Fig.1), supplemented with observational meta data – object identifier, observatory, measurement identifier, instrument/-band/filter/observing

mode, start/end time of the observations, duration, measured in-band flux (calibrated, aperture-/beam-corrected, non-linearity/saturation-corrected, etc.). 'Raw' flux densities/errors and observational meta data are typically available in the catalogues or target-specific papers where we take our basic data from. These papers/catalogues are listed in Sect. 5. All these flux densities are processed (e.g. converted to [Jy] from magnitudes), and brought to a common format along with all meta data in our processing (see also Fig.1).

We aim to include near-Earth, main-belt, and trans-Neptunian objects, all targets with significant amounts of thermal measurements from different satellite missions (IRAS, MSX, ISO, AKARI, Spitzer, Herschel, WISE, NEOWISE), from SOFIA, and from ground. In the current release (Public Release 1.0, PR1.0) we include IRAS, MSX, AKARI and WISE/NEOWISE observations. ISO, Spitzer and Herschel observations will be included in the upcoming releases.

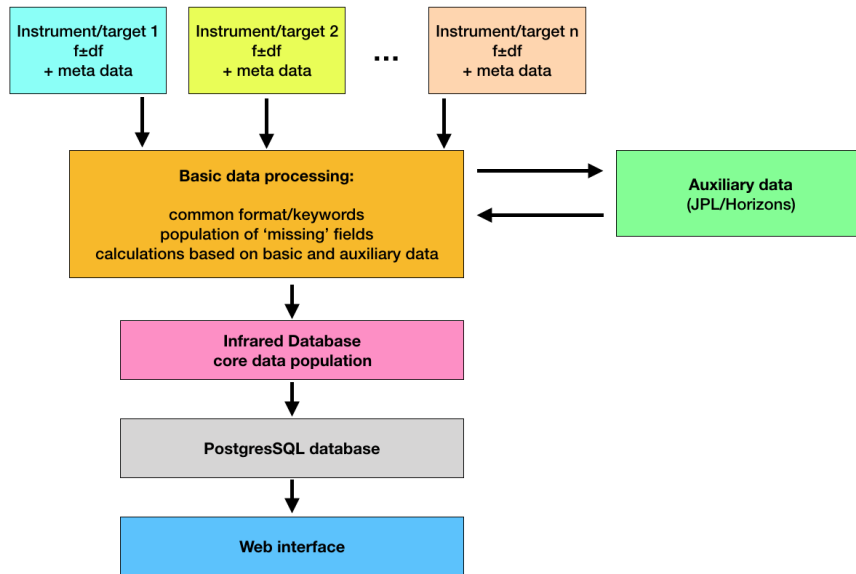


Figure 1: Outline of the processing of data from the basic entries (catalogues and target-specific papers) to the web-interface of the SBNaf infrared database.

To fully utilize these measurements we collect auxiliary data for the observations from external sources. These data are partly stored as additional useful entries (e.g. orbital elements and coordinates from JPL/Horizons) or used to calculate quantities that are necessary for the correct interpretation of the measurements (e.g. colour correction). A list of quality comments or other flags are also included.

The database is accessible through the webpage: <https://ird.konkoly.hu>, and the public website of the SBNaf H2020 project is: <http://www.mpe.mpg.de/~tmueller/sbnaf/>.

In the next sections we describe the additional data that we supplement the basic information with (Sect. 3), and give a detailed description of the database and its web interface in Sect. 4.

### 3 Auxiliary data

In addition to the measured flux and error, it is also necessary to calculate the monochromatic flux density at pre-defined reference wavelengths, to translate calendar dates to Julian date (JD, with/without correction for light-travel time), to convert wavelengths to frequencies, and to add absolute flux density errors. Below we summarized the main procedures to obtain these calculated values.

**Obtaining monochromatic flux density (colour correction):** For most of the instruments/filters included in the IRDB colour correction is calculated using the relative response profiles of the specific filters and assuming an estimated effective temperature ( $T_{\text{eff}}$ ) for the target, which is calculated as (Lang, 1999):

$$T_{\text{eff}} = \frac{392 K}{\sqrt{r_h}} (1 - p_V \cdot q)^{1/4} \quad (1)$$

, where  $r_h$  is the heliocentric distance (AU),  $p_V$  is the V-band geometric albedo and  $q$  is the standard *Bowell et al. (1989)* phase integral:  $q = 0.290 + 0.684G$ , where  $G$  is the slope parameter. If  $p_V$  is unknown/uncertain, we use  $p_V = 0.10$ . The colour corrected or monochromatic flux density is obtained as  $f_\lambda = f_i / K(\lambda)$ , where  $f_i$  is the in-band flux density obtained directly from the measurements and  $K(\lambda)$  is the colour correction factor, which is obtained using the spectral energy distribution of the source (flux density  $F_\nu(\lambda)$ ) and the relative response of the detector/filter system ( $R_\nu(\lambda)$ ) as:

$$K(\lambda) = \frac{\frac{1}{F_\nu(\lambda_c)} \int F_\nu(\lambda_c) R_\nu(\lambda_c) d\lambda}{\frac{1}{F_\nu^{ref}(\lambda_c)} \int F_\nu^{ref}(\lambda) R_\nu(\lambda) d\lambda} \quad (2)$$

where  $\lambda_c$  is the central (reference) wavelength of the filter in the photometric system and  $F_\nu^{ref}(\lambda)$  is the reference spectral energy distribution of the photometric system (typically  $\nu F_\nu = \text{const.}$  or Vega)

The monochromatic flux density uncertainties are calculated as:

$$\delta f_\lambda = \sqrt{\frac{1}{K(\lambda)^2} (\Delta f_i^2 + (r_{abs} f_i)^2) + (r_{cc} f_\lambda)^2} \quad (3)$$

where  $\Delta f_i$  is the in-band flux density uncertainty and  $r_{abs}$  is the absolute calibration error, usually expressed as a fraction of the in-band flux (see below). The last term contains the flux density uncertainty due to the colour correction uncertainty characterised by  $r_{cc}$ , which is approximately proportional to the deviation of the actual value of the colour correction from unity. In the present version it is implemented in the following way:

- if  $0.95 \leq K(\lambda) \leq 1.05$  then  $r_{cc} = 0.01$ ;
- if  $0.90 \leq K(\lambda) \leq 0.95$  then  $r_{cc} = 0.02$ ;
- if  $K(\lambda) \leq 0.90$  or  $K(\lambda) \geq 1.05$  then  $r_{cc} = 0.03$ ;

**Procedure for adding absolute calibration error:** Absolute calibration error is calculated as described above in Eq. 3. The  $r_{abs}$  factor is instrument/filter dependent and is determined during the flux calibration of the instrument and is described in instrument specific calibration papers. E.g. these  $r_{abs}$  values are 10%, 10%, 15% and 15% for the 12, 25, 60 and 100  $\mu\text{m}$  IRAS bands, respectively (Tedesco et al., 2002).

**JPL Horizons data:** Our database uses data obtained from NASA’s JPL-Horizons service. These information are stored in the database and available directly in the IRDB, and in some cases also used for further calculations. We query the following parameters from JPL-Horizons:

- Orbital elements: Semi-major axis,  $a$  (AU); eccentricity,  $e$ ; inclination w.r.t XY-plane,  $i$  (degrees) (XY-plane: plane of the Earth’s orbit at the reference epoch<sup>1</sup>; longitude of ascending node,  $\Omega$  (degrees); argument of perifocus,  $\varpi$  (degrees); mean anomaly,  $M$  (degrees).
- Parameters related to size and albedo: absolute magnitude,  $H$  (mag); slope parameter  $G$ ; object’s effective radius [km]; object’s V-band geometric albedo.
- Apparent position: Apparent right ascension (R.A.) and declination (DEC) at the time of the observation, ICRF/J2000 inertial reference frame, compensated for down-leg light-time [deg/deg]; rate of change of target center apparent R.A. and DEC (airless), note that  $dRA/dt$  is multiplied by the cosine of the declination [both in arcsec hour<sup>-1</sup>].
- Target brightness: Asteroid’s approximate apparent visual magnitude and surface brightness:  $APmag = H + 5 \cdot \log_{10}(\delta) + 5 \cdot \log_{10}(r) - 2.5 \cdot \log_{10}((1-G) \cdot \phi_1 + G \cdot \phi_2)$  [mag, mag arcsec<sup>-2</sup>].
- Heliocentric distance: Heliocentric range (“r”, light-time corrected) and range-rate (“rdot”) of the target center [AU and km s<sup>-1</sup>]. In addition, the one-way down-leg light-time from target center to observer is also retrieved [sec].
- Sun-Observer-Target angle: target’s apparent solar elongation seen from the observer location at print-time [degrees]. ‘/r’ flag indicating the target’s apparent position relative to the Sun in the observer’s sky (‘/T’ for trailing, ‘/L’ for leading).
- Ecliptic coordinates of the target: Observer-centered Earth ecliptic-of-date longitude and latitude of the target center’s apparent position, adjusted for light-time, the gravitational deflection of light and stellar aberration [deg/deg].
- X, Y, Z ecliptic J2000 cartesian coordinates (Archinal et al. 2011) of the target as seen from the sun’s centre/observer’s position in au (see Table 1). These coordinates also allow us to combine remote with close proximity measurements (e.g. Bennu and Ryugu), provided that the implementation of the spacecraft trajectories are correctly implemented in JPL/Horizons.

## 4 Database and access

### 4.1 Main database file and web interface

From the collected data (flux densities, observational meta data and auxiliary data, see above) a PostgreSQL table is created that is the essentially the SBNAF Infrared Database. The database is accessible through a web interface, available at <https://ird.konkoly.hu>. An example is shown below, presenting the query screen and the resulting output screen for some selected IRAS and AKARI observations of 1 Ceres.

The user of the webpage can generate a query following the instructions given here in this document or following the examples on the IRDB webpage. The results are generated on the screen as

---

<sup>1</sup>obliquity of 84381.448 arcseconds wrt ICRF equator (IAU76)

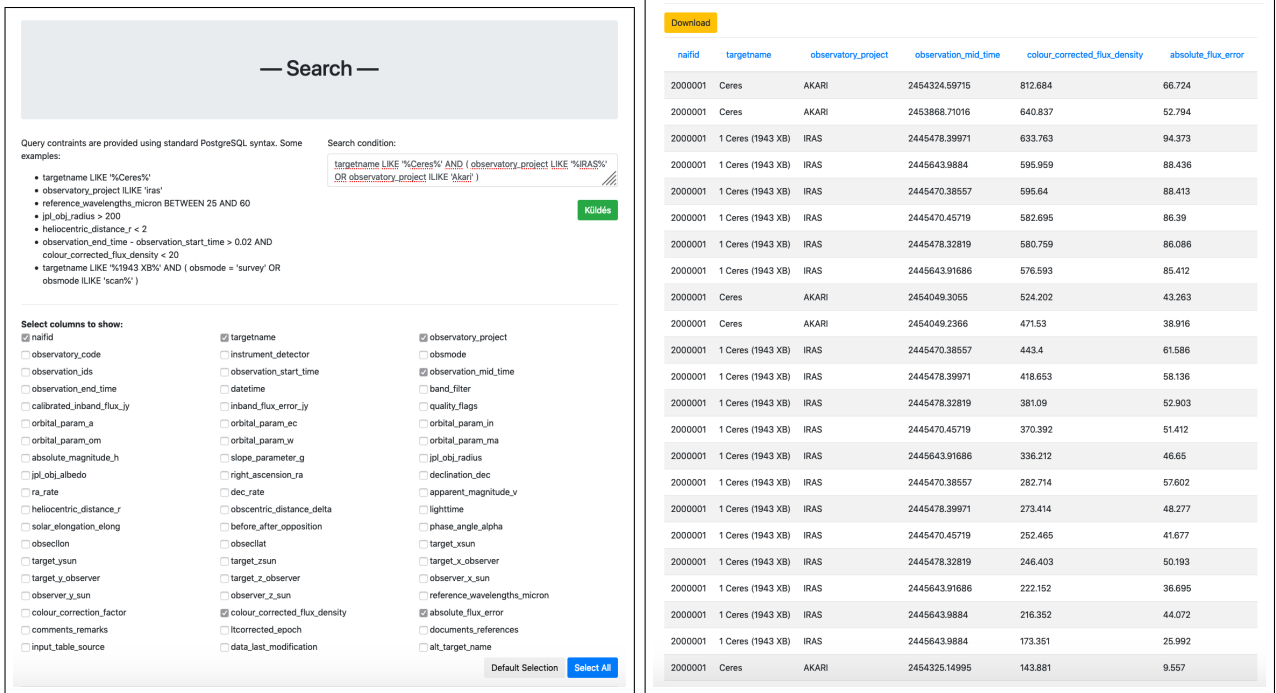


Figure 2: Query and results listing infrared observation of 1 Ceres and displaying the default output selection: 'naifid', 'targetname', 'observatory\_project', 'observation\_mid\_time', 'colour\_corrected\_flux\_density', and 'absolute\_flux\_error'.

HTML tables, but the user has the option to download the output page as a .csv file ("Download" button).

The example above was generated by the following query: **targetname LIKE '%Ceres%' AND ( observatory\_project LIKE 'IRAS' OR observatory\_project ILIKE 'AKARI' )**, requiring exact, case sensitive matching with 'LIKE' on 'targetname' (= 'Ceres') and selecting observatories 'IRAS' (exact name again with 'LIKE') and 'AKARI' (selecting with 'ILIKE', i.e. case-insensitive). In this case the output gives the default selection: 'naifid', 'targetname', 'observatory\_project', 'observation\_mid\_time', 'colour\_corrected\_flux\_density', and 'absolute\_flux\_error'. Note the capital letters (AND, OR, etc.), and the extra single spaces between the brackets and the text in the query specification.

Numeric data types (FLOAT, DOUBLE) can be queried as follows: **observation\_start\_time BETWEEN 2453869 AND 2454000**: selects the objects where the observation time started between 2453869 and 2454000 (JD); **observation\_start\_time > 2453869 AND observation\_start\_time < 2454000**: returns the same results as the previous query. **naifid = 2000001**: returns all targets with 'naifid' exactly equal to 2000001.

For string type data: **targetname ILIKE '%ceres%'**: selects the targets with the substring "ceres" in it, case insensitive; **observatory\_project = 'IRAS'**: returns all observations where the observatory\_project name matches 'IRAS' exactly.

The query **"comments\_remarks ILIKE '%comet%'"** lists measurements of comets (currently the AKARI observations of the comet P/2006 HR30 (Siding Spring) in the D2.5 version of the database).

Mission	JPL code	instrument	filters	observing mode	$N_{obs}$
AKARI	500@399	IRC-NIR	N4	IRC02	1
		IRC-MIR-S	S7, S9W, S11	survey, IRC02, IRC11	6955
		IRC-MIR-L	L15, L18W, L24	survey, IRC02, IRC51	13824
HSO	500@-486	PACS	blue,green,red	chop-nod, scan map	2333
MSX	500@399	MSX_A,MSX_C,MSX_D,MSX_E		survey	901
IRAS	500@399	IRAS12,IRAS25,IRAS60,IRAS100		survey	25064
WISE	500@-163	W3,W4		survey	121383

Table 1: List of observatories/missions, observatory codes, instruments, filters, possible observing modes, and the number of measurements with a specific instrument, in the present version of the Infrared Database. Except for WISE, there are no available positions for the low-Earth orbit missions, so they are referred to as geocentric (JPL code ‘500@399’).

Additional examples are given on the starting page of the web interface.

## 4.2 Alternative access to the database

Our database is accessible via the VESPA (Erard et al., 2018) query interface at <http://vespa.obspm.fr/planetary/data/>. If your target is in our database, you can find the entries after your search. If you want to directly make a query in our database through VESPA, search for the SBNAF service in the list of EPN Resources.

Alternatively, the database is available via the standard Table Access Protocol (TAP) at <http://nadir.konkoly.hu:80/tap>. You can use any compatible VO tool to access it, e.g. TOPCAT.

## 4.3 Summary of database fields

Below we give a description of the output fields of the Infrared Database. The unit and the data type of the specific field are given in squared and regular brackets, respectively.

**naifid:** NASA’s Navigation and Ancillary Information Facility<sup>2</sup> Solar System object code of the target (LONG)

**targetname:** The name of the asteroid, with number and possible alternative designations, if available (STRING)

**alt\_target\_name:** Alternative designation(s) of the asteroid, e.g. provisional designation, separated by “#”, if multiple (STRING)

**observatory\_project:** Name of the observatory/ space mission (STRING). The possible values are for the current release: ‘IRAS’: Infrared Astronomy Satellite; ‘AKARI’: AKARI Space Telescope; ‘MSX’: Midcourse Space Experiment; ‘WISE’: Wide-field Infrared Survey Explorer; ‘HSO’: Herschel Space Observatory.

See Table1 for a list of instruments, filters and observatory codes used in this database. References for the listed instruments and flux density measurements can be found in Sect. 5.

<sup>2</sup>[https://naif.jpl.nasa.gov/pub/naif/toolkit\\_docs/FORTRAN/req/naif.ids.html](https://naif.jpl.nasa.gov/pub/naif/toolkit_docs/FORTRAN/req/naif.ids.html)

**observatory\_code:** JPL/Horizons code of the observatory/spacecraft, see Table 1 for a list (STRING)

**instrument\_detector:** Instrument of the observatory/spacecraft used in that specific measurement, see Table 1 for a list (STRING) (STRING)

**obsmode:** Observation mode, also listed in Table 1. For a description of the observing modes, see the respective references of the instruments in Sect. 5. For instruments working in survey mode (like IRAS and MSX) with which no pointed observations were possible and data are taken from the survey data 'survey' in the 'obsmode' column indicates the default observing mode (STRING)

**observation\_IDs:** Mission-specific identifier of the observation, e.g. *OBSID* for Herschel measurements and *AORKEY* for Spitzer observations [unitless] (STRING)

**observation\_start\_time** Start time of the measurement [Julian date] (DOUBLE)

**observation\_mid\_time** Mid-time of the measurement [Julian date] (DOUBLE)

**observation\_end\_time** End time of the measurement [Julian date] (DOUBLE)

**datetime** Observation date in the format 'YYYY:MM:DD hh:mm:ss.sss', with YYYY: year; MM: month in string format (Jan, Feb, etc.), DD: day of the month; hh: hour of the day; mm: minutes; ss.sss: seconds with three-digit accuracy (STRING)

**band\_filter** Name of the filter/band used for the specific observation (STRING)

**calibrated\_inband\_flux\_Jy:** In-band photometric flux density in [Jansky] units, with all photometric corrections applied, including aperture/encircled energy fraction corrections, but without colour correction (DOUBLE). Sources of original data are listed in Sect. 5.

**inband\_flux\_error\_Jy:** Uncertainty of the in-band photometric flux density 'calibrated\_inband\_flux\_Jy', with all direct photometric errors considered, but without errors related to the spectral energy distribution of the target (colour correction), and also without the consideration of the absolute photometric error of the instrument (DOUBLE).

**quality\_flags:** (STRING)

- WISE<sup>3</sup>:

- Contamination and confusion flags:

- \* P - Persistence. Source may be a spurious detection of (P).

- \* p - Persistence. Contaminated by (p) a short-term latent image left by a bright source.

- \* 0 (number zero) - Source is unaffected by known artifacts.

---

<sup>3</sup><http://wise2.ipac.caltech.edu/docs/release/allsky/expsup/index.html>

– Photometric quality flags:

\* A - Source is detected in this band with a flux signal-to-noise ratio  $w\_snr > 10$ .

\* B - Source is detected in this band with a flux signal-to-noise ratio  $3 < w\_snr < 10$ .

**orbital\_param\_A:** Semi-major axis of the target’s orbit, as obtained from JPL/Horizons [AU] (DOUBLE)

**orbital\_param\_EC:** Eccentricity of the target’s orbit, as obtained from JPL/Horizons [unitless] (DOUBLE)

**orbital\_param\_IN:** Inclination of the target’s orbit, as obtained from JPL/Horizons [deg] (DOUBLE)

**orbital\_param\_OM:** Longitude of the ascending node of the target’s orbit, as obtained from JPL/Horizons [deg] (DOUBLE)

**orbital\_param\_W:** Argument of the periapsis of the target’s orbit, as obtained from JPL/Horizons [deg] (DOUBLE)

**orbital\_param\_MA:** The mean anomaly of the target’s orbit, as obtained from JPL/Horizons [deg] (DOUBLE)

**absolute\_magnitude\_H** The absolute magnitude of the target, i.e. the visual magnitude an observer would record if the asteroid were placed 1 AU away, and 1 AU from the Sun and at a zero phase angle, as obtained from JPL/Horizons [mag] (FLOAT)

**slope\_parameter\_G** ‘G’ slope parameter of the target, describing the dependence of the apparent brightness on the phase angle (light scattering on the asteroid’s surface); for more details, see Bowel (1989) (FLOAT)

**jpl\_obj\_radius:** Estimated radius of the target as obtained from JPL Horizons [km] (FLOAT)

**jpl\_obj\_albedo:** Estimated V-band geometric albedo of the target as obtained from JPL Horizons (FLOAT)

**Right\_Ascension\_RA:** Right ascension (J2000) of the target at observation mid-time, calculated from the orbit by JPL/Horizons [deg] (FLOAT)

**Declination\_DEC:** Declination (J2000) of the target at observation mid-time, calculated from the orbit by JPL/Horizons [deg] (FLOAT)

**RA\_rate:** The rate of change in right ascension [ $\text{arcsec s}^{-1} \equiv \text{deg h}^{-1}$ ] (FLOAT)

**DEC\_rate** The rate of change in declination [ $\text{arcsec s}^{-1} \equiv \text{deg h}^{-1}$ ] (FLOAT)

**apparent\_magnitude\_V** Estimated apparent brightness of the target in V-band at observation mid-time, as obtained by JPL/Horizons [mag] (FLOAT)

**heliocentric\_distance\_r**: Heliocentric distance of the target at observation mid-time, as obtained by JPL/Horizons [AU] (DOUBLE)

**obscentric\_distance\_delta**: Observer to target distance at observation mid-time, as obtained by JPL/Horizons [AU] (DOUBLE)

**lighttime**: The elapsed time since light (observed at print-time) would have left or reflected off a point at the center of the target [sec] (FLOAT)

**solar\_elongation\_elong**: Target's apparent solar elongation seen from the observer location at print-time, in degrees (FLOAT)

**before\_after\_opposition**: A flag regarding the target's apparent position relative to the Sun in the observer's sky. '/T' indicates trailing, '/L' leading position with respect to the Sun (STRING)

**phase\_angle\_alpha**: The Sun-Target-Observer angle at observation mid-time, as obtained by JPL/Horizons [deg] (FLOAT)

**ObsEclLon/ObsEclLat**: Observer-centered Earth ecliptic-of-date longitude and latitude of the target center's apparent position, adjusted for light-time, the gravitational deflection of light and stellar aberration, in degrees, as obtained by JPL/Horizons [deg] (FLOAT)

**target\_[X,Y,Z]@sun** Sun-centered X, Y, Z Cartesian coordinates of the target body at observation mid-time, in the reference frame defined in Archinal et al. (2011) [AU]. (DOUBLE)

**target\_[X,Y,Z]\_@observer**: Observer-centered X, Y, Z Cartesian coordinates of the target body at observation mid-time, in the reference frame defined in Archinal et al. (2011) [AU]. (DOUBLE)

**observer\_[X,Y,Z]\_@sun** Sun-centered X, Y, Z Cartesian coordinates of the observer at observation mid-time, in the reference frame defined in Archinal et al. (2011) [AU]. (DOUBLE) (DOUBLE)

**reference\_wavelengths\_micron** Reference wavelength of the measuring filter in [ $\mu\text{m}$ ] units (FLOAT)

**colour\_correction\_factor** Colour correction factor applied to obtain monochromatic flux density from in-band flux density [unitless]; see Sect. 3 for details (FLOAT)

**colour\_corrected\_flux\_density**: Monochromatic flux density (colour corrected in-band flux density) [Jy]; see Sect. 3 for details (DOUBLE)

**absolute\_flux\_error**: Absolute uncertainty of the monochromatic flux density including the uncertainty of the absolute flux calibration [Jy]; see Sect. 3 for details (DOUBLE)

**comments\_remarks:** Comments regarding the quality of the measurement / information when an assumed value was applied in the calculations; indicating whether the target is (also) regarded as a comet in JPL/Horizons (STRING)

**LTcorrected\_epoch:** The lighttime corrected epoch, calculated as  $observation\_mid\_time - lighttime/3600./24$ . [day] (DOUBLE)

**documents\_references:** Publications/resources where the photometric data were taken from (STRING). A list of codes can be found in Sect. 5.

**input\_table\_source:** Name of the input file which the database was generated from (strictly for internal usage) (STRING)

**data\_last\_modification:** The date when the record was last modified, in 'human readable' format: 'YYYY-MMM-DD hh:mm:ss' (STRING)

## 5 Key references and sources of data

Below we give a summary of the references and sources of asteroid flux densities related to each mission/telescope. A simple reference code is also given for the those papers or catalogues that presented flux densities used for our database. These codes are listed in the '*documents\_references*' field of the database for each measurement.

**IRAS:** A general description of the Infrared Astronomical Satellite (IRAS) mission can be found in (Neugebauer et al., 1984). A detailed summary of the IRAS mission is given in the IRAS Explanatory Supplement, available at the NASA/IPAC Infrared Science Archive (<http://irsa.ipac.caltech.edu/IRASdocs/exp.sup/>), that also covers calibration issues (point source calibration, estimated accuracy, bright source problems, colour correction).

Asteroid fluxes are obtained from 'The Supplemental IRAS Minor Planet Survey' (Tedesco et al., 2002) [**T02IRAS**].

**MSX:** Mill (1994) and Mill et al. (1994) provide an overview of the spacecraft, its instruments, and scientific objectives, and Price & Witteborn (1995) and Price et al. (1998) a general description of the astronomy experiments. More details on the astronomy experiments and the influence the spacecraft design has on these experiments may be found in Price et al. (2001).

Asteroid fluxes are obtained from 'The Midcourse Space Experiment Infrared Minor Planet Survey' catalogue (Tedesco et al., 2002b) [**T02MSX**].

**AKARI:** The AKARI mission is described in (Murakami et al., 2007).

Minor planet flux densities are obtained from the AKARI Asteroid Flux Catalog Ver.1<sup>4</sup> (Release October 2016), referred to as [**AKARIAFC**] in the IRDB. The catalogue contains data from the all-sky survey (Usui et al., 2011), slow-scan observation (Hasegawa et al., 2013), and pointed observations of (25143) Itokawa and (162173) Ryugu (Müller et al., 2017). These 'non-survey' modes have their

---

<sup>4</sup>[https://www.ir.isas.jaxa.jp/AKARI/Archive/Catalogues/Asteroid\\_Flux\\_V1/](https://www.ir.isas.jaxa.jp/AKARI/Archive/Catalogues/Asteroid_Flux_V1/)

special flags in the 'obsmode' fields (IRC02: pointed observations; IRC11/IRC51: slow scan), as defined in the AKARI Asteroid Flux Catalogue.

**Herschel:** The Herschel Space Observatory mission is summarized in (Pilbratt et al., 2010). The PACS instrument (Photometer Array Camera and Spectrometer) is described in Poglitsch et al. (2010). The photometric calibration of PACS is discussed in ? (chop-nod photometric observing mode) and in (?).

Flux densities of Solar System small bodies are obtained from some selected publications for near-Earth asteroids and Centaurs/transneptunian objects ([D14]).

- Near-Earth asteroids:
  - Müller et al. (2012) [M12]: (101955) Bennu
  - Müller et al. (2017) [M13]: (308625) 2005 YU55
  - Müller et al. (2017) [M14]: (99942) Apophis
  - Müller et al. (2017) [M17]: (162173) Ryugu
- Centaurs and transneptunian objects:
  - Duffard et al. (2014) [D14]: 16 Centaurs
  - Fornasier et al. (2013) [F13]: (2060) Chiron, (10199) Chariklo, (38628) Huya, (50000) Quaoar, (55637) 2002 UX25, (84522) 2002 TC302, (90482) Orcus, (120347) Salacia, (136108) Haumea
  - Farkas-Takács et al. (2020) [FT20]: 23 resonant transneptunian and scattered disk objects
  - Kiss et al. (2013) [K13]: 2012 DR30
  - Lellouch et al. (2010) [L10]: (136108) Haumea
  - Lellouch et al. (2013) [L13]: (20000) Varuna, (55636) 2002 TX300, (120348) 2004 TY364, (15820) 1994 TB, (28978) Ixion (33340) 1998 VG44, (26308) 1998 SM165, (26375) 1999 DE9, (119979) 2002 WC19, (44594) 1999 OX3, (48639) 1995 TL8
  - Lellouch et al. (2016) [L16]: Pluto and Charon
  - Lim et al. (2010) [LIM10]: (136472) Makemake
  - Mommert et al. (2012) [MM12]: 18 plutinos
  - Müller et al. (2010) [M10]: (208996) 2003 AZ84, (126154) 2001 YH140, (79360) Sila-Nunam, (82075) 2000 YW134, (42355) Typhon, 2006 SX368, (145480) 2005 TB190
  - Müller et al. (2019) [M19A]: (136081) Haumea
  - Pál et al (2012) [P12]: (90377) Sedna and 2010 EK139
  - Pál et al. (2015) [P15]: 2013 AZ60
  - Santos-Sanz et al. (2012) [SS12]: 15 scattered disk and detached objects
  - Santos-Sanz et al. (2017) [SS17]: (84922) 2003 VS2, (208996) 2003 AZ84
  - Vilenius et al. (2012) [V12]: 19 classical transneptunian objects
  - Vilenius et al. (2014) [V14]: 18 classical transneptunian objects
  - Vilenius et al. (2018) [V18]: 1995 SM55, 2005 RR43, 2003 UZ117, 2003 OP32, 2002 TX300, 1996 TO66, 1999 CD158, 1999 KR16

**WISE:** The WISE mission is described in (Wright et al., 2010). Data products are summarized in the 'Explanatory Supplement to the AllWISE Data Release Products' (Cutri et al., 2013).

The WISE Moving Object Pipeline Subsystem (WMOPS) reported all detections of Solar System small bodies to the IAU Minor Planet Center (MPC) for confirmation, whereas the computed in-band magnitudes were collected in the IRSA/IPAC archive, namely in the Level 1b catalogues. To retrieve these magnitudes, we queried the IPAC archive using a 1 arcsec cone search radius around the MPC-reported tracklets, which are all labelled "C51" by the MPC. This way we avoid using false detections that may have been included in the IPAC archive (Mainzer et al. 2011).

Since we are only interested in flux densities collected during the fully-cryogenic phase of the mission, we queried the WISE All-Sky Database. The in-band magnitudes ( $m$ ) were converted to in-band flux densities ( $\langle f \rangle$ ) as:

$$\langle f \rangle = \langle f_0 \rangle 10^{-0.4m} \quad (4)$$

where  $\langle f_0 \rangle$  is the zero-magnitude isophotal flux density of Vega for each band, as reported in Wright et al. (2010). By definition,  $\langle f_0 \rangle$  does not require a colour correction. From the tabulated magnitude error bar  $\Delta m$ , the corresponding error bar of the in-band flux is given by:

$$\Delta f = 0.40 \log_{10} \langle f \rangle \Delta m \quad (5)$$

To correct for a discrepancy between red and blue calibrators observed after launch, Wright et al. suggest shifting the W3 and W4 isophotal wavelengths and correcting the isophotal flux densities accordingly. Thus, we took 11.10 and 22.64  $\mu\text{m}$  and 31.37 and 7.952 Jy, respectively (more details in Masiero et al. 2011). Flux densities obtained using this procedure are referred to as [**WISEASD**] in the respective field of our IRDB.

## References

- Archinal, B., A'Hearn, M.F., Bowell, E., et al., 2011, *CeMDA*, 109, 101
- Beichman, C. A.; Neugebauer, G.; Habing, H. J.; Clegg, P. E.; Chester, Thomas J., 1988, *Infrared astronomical satellite (IRAS) catalogs and atlases. Volume 1: Explanatory supplement*, California Institute of Technology, Pasadena
- Bowell E.G., Hapke B., Domingue D., Lumme K., Peltoniemi J., and Harris A.W., 1989, Application of photometric models to asteroids. In *Asteroids II*, edited by T. Gehrels, M. T. Matthews, R.P. Binzel, University of Arizona Press, pp. 524–555.
- Cutri, R. M.; Wright, E. L.; Conrow, T., et al., 2013, *Explanatory Supplement to the WISE All-Sky Data Release Products*
- Duffard, R., Pinilla-Alonso, N., Santos-Sanz, P., et al., 2014, *A&A*, 564, A92 [D14]
- Erard, S., Cecconi, B., Le Sidaner, P., et al., 2018, *P&SS*, 150, 65E
- Farkas-Takács, A., Kiss, Cs., Vilenius, E., et al., 2020, *A&A* 638, A23 [FT20]
- Fornasier, S., Lellouch, E., Müller, T., et al., 2013, *A&A*, 555, A15 [F13]
- Hasegawa, S., Müller, Th.G., Kuroda, D., Takita, S., Usui, F., 2013, *Publications of the Astronomical Society of Japan*, 65, id.34
- Kiss, Cs., Szabó, Gy.; Horner, J., et al., 2013, *A&A*, 555, A3 [K13]
- Kiss, C.; Müller, T. G.; Vilenius, E.; et al., 2014, *Experimental Astronomy*, 37, 161
- Lang, K. R., 1999, *Astrophysical formulae*, New York:Springer, 1999. *Astronomy and astrophysics library*, ISSN0941-7834
- Lellouch, E., Kiss, Cs., Santos-Sanz, P., et al., 2010, *A&A*, 518, L147
- Lellouch, E., Santos-Sanz, P., Lacerda, P., et al., 2013, *A&A*, 557, A60
- Lim, T. L., Stansberry, J., Müller, T.G., et al., 2010, *A&A*, 518, L148
- Mainzer, A.; Grav, T.; Bauer, J., et al., 2011, *ApJ*, 743, 156
- Mainzer, A. K., Bauer, J. M., Cutri, R. M., et al., 2016, 'NEOWISE Diameters and Albedos V1.0', NASA Planetary Data System, id. EAR-A-COMPIL-5-NEOWISEDIAM-V1.0
- Masiero, J.; Mainzer, A.; Grav, T.; et al., 2011, *The Astrophysical Journal*, 741, id.68
- Mill, J.D., 1994, "Midcourse Space Experiment (MSX): an overview of the instruments and data collection plans", *Proc. SPIE* 2232, 200
- Mill, John D.; O'Neil, Robert R.; Price, Stephan, et al., 1994, *Journal of Spacecraft and Rockets*, 31, 900
- Müller, T. G.; O'Rourke, L.; Barucci, A. M.; et al., 2012, *A&A*, 548, A36 [M12]
- Müller, T. G.; Miyata, T.; Kiss, C.; et al., 2013, *A&A*, 558, A97 [M13]
- Müller, T. G., Kiss, C., Scheirich, P., et al., 2014, *A&A*, 566, A22 [M14]
- Müller, Th.G., Hasegawa, S., Usui, F., 2014, *Publications of the Astronomical Society of Japan*, 66, id.5217
- Müller, Th.G.; Durech, J., Ishiguro, M., 2017, *Astronomy & Astrophysics*, 599, id.A103
- Müller et al., 2019, in prep. [M19A]
- Müller et al., 2019, in prep. [M19B]
- Murakami, H., Baba, H., Barthel, P., et al., 2007, *Publications of the Astronomical Society of Japan*, 59, S369

- Neugebauer, G., Habing, H. J., van Duinen, R. et al. 1984, *The Astrophysical Journal*, 278, 1
- Pál, A.; Kiss, C.; Müller, T. G., et al., 2012, *A&A*, 541, L6 [P12]
- Pál, A.; Kiss, Cs.; Horner, J., et al., 20015, *A&A*, 583, A93 [P15]
- Pilbratt, G. L., Riedinger, J. R., Passvogel, T., et al.,
- Poglitsch, A., Waelkens, C., Geis, N., et al., 2010, *A&A*, 518, L2
- Price, S. D.; Witteborn, F. C., 1995, 'MSX Mission Summary', *Astronomical Society of the Pacific Conference Series*, Volume 73, LC # QB470.A1 A37, p.685
- Price, S. D.; Tedesco, E. F.; Cohen, M.; et al., 1998, 'Astronomy on the Midcourse Space Experiment', *New Horizons from Multi-Wavelength Sky Surveys*, *Proceedings of the 179th Symposium of the International Astronomical Union*, held in Baltimore, USA August 26-30, 1996, Kluwer Academic Publishers, edited by Brian J. McLean, Daniel A. Golombek, Jeffrey J. E. Hayes, and Harry E. Payne, p. 115.
- Price, Stephan D.; Egan, Michael P.; Carey, Sean J.; Mizuno, Donald R.; Kuchar, Thomas A., 2001, *The Astronomical Journal*, 121, 2819
- Tedesco, E. F., Noah, P. V., Noah, M., Price S. D. 2002, *Astronomical Journal*, 123, 1056 [T02IRAS]
- Tedesco, E. F., Egan, M. P., Price S. D. 2002b, *Astronomical Journal*, 124, 583 [T02MSX]
- Usui, F., Kuroda, D., Müller, Th.G., et al., 2011, *Publications of the Astronomical Society of Japan*, 63, 1117
- Vilenius, E., Kiss, Cs., Mommert, M., et al., 2012, *A&A*, 541, A94
- Vilenius, E., Kiss, Cs., Müller, T.G., et al., 2014, *A&A*, 564, A35
- Vilenius, E., Stansberry, J., Müller, T., et al., 2018, *A&A*, 618, A136 [V18]
- Wright, E.L.; Eisenhardt, P.R.M.; Mainzer, A.K., 2010, *The Astronomical Journal*, 140, 1868

# Appendix

Below we present the specification of the infrared database fields through an example (AKARI measurement of (25143) Itokawa), as it was at the time of the production of this document. Changes may apply and will be reported in the next release note of the database.

Parameter	Type	Unit	ExampleValue	Retrieved from JPL
01 naifid	LONG	---	2025143	No
02 targetname	STRING	---	25143 Itokawa (1998 SF36)	No
03 observatory_project	STRING	---	AKARI	No
04 observatory_code	STRING	---	5008399	No
05 instrument_detector	STRING	---	IRC-MIR-L	No
06 obsmode	STRING	---	IRC02	No
07 observation_IDs	STRING	---		No
08 observation_start_time	DOUBLE	days	2454308.04699	No
09 observation_mid_time	DOUBLE	days	2454308.04699	No
10 observation_end_time	DOUBLE	days	2454308.04699	No
11 datetime	STRING	---	2007-Jul-26 13:07:40.000	No
12 band_filter	STRING	---	L15	No
13 calibrated_inband_flux_Jy	DOUBLE	Jy	0.02	No
14 inband_flux_error_Jy	DOUBLE	Jy	0.001	No
15 quality_flags	STRING	---		No
16 orbital_param_A	DOUBLE	au	1.32404449	Yes
17 orbital_param_EC	DOUBLE	---	0.28018482	Yes
18 orbital_param_IN	DOUBLE	deg	1.62206524	Yes
19 orbital_param_OM	DOUBLE	deg	69.09531692	Yes
20 orbital_param_W	DOUBLE	deg	162.77163687	Yes
21 orbital_param_MA	DOUBLE	deg	32.28481921	Yes
22 absolute_magnitude_H	FLOAT	mag	19.2	Yes
23 slope_parameter_G	FLOAT	---	0.15	Yes
24 jpl_obj_radius	FLOAT	km	0.165	Yes
25 jpl_obj_albedo	FLOAT	---	0.1	Yes
26 Right_Ascension_RA	FLOAT	deg	209.5522	Yes
27 Declination_DEC	FLOAT	deg	-16.11449	Yes
28 RA_rate	FLOAT	"/sec	0.0654038 (JPL/horizons gives "/hour!)	Yes
29 DEC_rate	FLOAT	"/sec	-0.028018 (JPL/horizons gives "/hour!)	Yes
30 apparent_magnitude_V	FLOAT	mag	19.16	Yes
31 heliocentric_distance_r	DOUBLE	au	1.05402381	Yes
32 obscentric_distance_delta	DOUBLE	au	0.28128128	Yes
33 lighttime	FLOAT	sec	140.3607	Yes
34 solar_elongation_elong	FLOAT	deg	90.0359	Yes
35 before_after_opposition	STRING	---	/T	Yes
36 phase_angle_alpha	FLOAT	deg	-74.49	Yes
37 ObsEclLon	FLOAT	deg	213.2239	Yes
38 ObsEclLat	FLOAT	deg	-3.795164	Yes
39 target_X_@sun	DOUBLE	au	0.319379555249375	Yes
40 target_Y_@sun	DOUBLE	au	-1.00430258867518	Yes
41 target_Z_@sun	DOUBLE	au	-0.0185976638442141	Yes
42 target_X_@observer	DOUBLE	au	-0.235047951829334	Yes
43 target_Y_@observer	DOUBLE	au	-0.153329693108554	Yes
44 target_Z_@observer	DOUBLE	au	-0.0186135080544228	Yes
45 observer_X_@sun	DOUBLE	au	0.554427507078709	Yes
46 observer_Y_@sun	DOUBLE	au	-0.850972895566624	Yes
47 observer_Z_@sun	DOUBLE	au	1.58442102086986E-05	Yes
48 reference_wavelengths_micron	FLOAT	micron	24.0	No
49 colour_correction_factor	FLOAT	---	0.984	No
50 colour_corrected_flux_density	DOUBLE	Jy	0.021	No
51 absolute_flux_error	DOUBLE	Jy	0.001	No
52 comments_remarks	STRING	---	An assumed geometric albedo of 0.1 was used to calculate the colour-correction factor.	No
53 LTcorrected_epoch	DOUBLE	days	2454308.045366 / to be calculated from (observation_mid_time - lighttime/3600./24.)	No
54 documents_references	STRING	---	Mueller T. G. et al. 2014;AKARIAFC	No
55 input_table_source	STRING	---	AKARI_allsky_wheader.csv	No
56 date_last_modification	STRING	---	2018-08-31 15:13:25	No